

# Asymmetric Nuclear Matter with Pion Dressing

S. Sarangi,<sup>1</sup> P. K. Panda,<sup>2</sup> S. K. Sahu,<sup>3</sup> and L. Maharana<sup>4</sup>

<sup>1</sup>*ICFAI Institute of Science & Technology, Bhubaneswar-751010, India*

<sup>2</sup>*Indian Association for the Cultivation of Sciences, Jadavpur, Kolkata-700 032, India*

<sup>3</sup>*Physics Department, Banki College, Banki-754008, Cuttack, India*

<sup>4</sup>*Physics Department, Utkal University, Bhubaneswar-751004, India\**

We discuss here a self-consistent method to calculate the properties of the cold asymmetric nuclear matter. The nuclear matter is dressed with  $s$ -wave pion pairs. The nucleon-nucleon (N-N) interaction is mediated by these pion pairs,  $\omega$  and  $\rho$  mesons. The parameters of these interactions are calculated self-consistently to obtain the saturation properties like equilibrium binding energy, pressure, compressibility and symmetry energy. The computed equation of state is then used in the Tolman- Oppenheimer-Volkoff (TOV) equation to study the mass and radius of a neutron star containing pure neutron matter.

PACS numbers: 21.65.+f, 21.30.Fe, 24.10.Cn, 26.60.+c

## I. INTRODUCTION

The properties of nuclear matter has been an area of considerable research interest for the past few decades. Such studies are of vital importance in nuclear physics, (e.g., in the context of nucleon-nucleon (N-N) interaction, structure and properties of finite nuclei, dynamics of heavy ion collisions), astrophysics (nucleosynthesis, structure and evolution of neutron stars [1] bordering on big-bang cosmology) and also particle physics (production and interaction among hadrons). An obvious special case of study has been the properties of symmetric nuclear matter. However, the more general study of asymmetric nuclear matter has been receiving considerable attention of late [2, 3, 4] due to its importance in prediction of properties of exotic nuclei, the reaction dynamics of heavy ion collisions, and properties of neutron stars.

One of the fundamental concerns in the study of nuclear matter is the nature of the N-N interaction. The residual N-N interaction arising from the nucleonic substructure of quarks and gluons is basically non-perturbative in nature. Therefore, the general approach is to self-consistently solve the problem, albeit in different ways. The different approaches can be broadly classified into three general types [5, 6], namely, the *ab initio* methods, the effective field theory approaches and calculations based on phenomenological density functionals. The *ab initio* methods include the Brueckner-Hartree-Fock (BHF) [7, 8, 9] approach, the (relativistic) Dirac-Brueckner-Hartree-Fock (DBHF) [10, 11, 12, 13, 14] calculations, the Green Function Monte-Carlo (GFMC) [15, 16, 17] method using the basic N-N interactions given by boson exchange potentials. The other approach of this type, also known as the variational approach, is pioneered by the Argonne Group [18, 19]. This method is also based on basic two-body (N-N) interactions in a non-relativistic formalism with relativistic corrections introduced at a later stage. The effective field theory (EFT) approaches are based on density functional theories [20, 21] like chiral perturbation theory [22, 23]. These calculations involve a few density dependent model parameters evaluated iteratively. The third type of approach, namely, the calculations based on phenomenological density functionals include models with effective density dependent interactions such as Gogny or Skyrme forces [24] and the relativistic mean field (RMF) models [25, 26, 27, 28, 29, 30, 31]. The parameters of these models are evaluated by appealing to the bulk properties of nuclear matter and properties of closed shell nuclei. Our work presented here belongs to this class of approaches although in the non-relativistic limit.

The RMF models represent the N-N interactions through the coupling of nucleons with isoscalar scalar  $\sigma$  mesons, isoscalar vector  $\omega$  mesons, isovector vector  $\rho$  mesons and the photon quanta besides the self- and cross-interactions among these mesons [28, 29, 30]. There have also been recent efforts to examine the role of isovector scalar  $\delta$  mesons [31]. Although implemented at Hartree level only, these models have been very successful in simulating the observed bulk properties of nuclear matter including the nuclear equation of state (EOS), mass and radii of neutron star as well as in explaining properties of finite nuclei [20, 24, 27]. Recently, the RMF theory has been extended to include the quasi-particle contributions in a relativistic continuum Hartree Bogoliubov theory [32] and applied to the study of exotic nuclei.

---

\*Electronic address: lmaharan@iopb.res.in

Nuclear equations of state have also been constructed using the quark meson coupling model (QMC) [33] where baryons are described as systems of non-overlapping MIT bags which interact through effective scalar and vector mean fields, very much in the same way as in the RMF model. The QMC model has also been applied to study the asymmetric nuclear matter at finite temperature [34].

It has been shown earlier [35, 36], that the medium and long range attraction effect provided by  $\sigma$  mesons in RMF theory can be simulated by  $s$ -wave pion pairs which provide the “dressing” to the nuclear matter. Similar dressing of pions have also been considered to study the properties of deuteron [37] and  ${}^4\text{He}$  [38]. On this basis, we start with a relativistic Lagrangian density with  $\pi N$  interaction. The short range repulsion and the isospin asymmetry part of the NN interaction are parametrized by two additional terms representing the coupling of nucleons with the  $\omega$  and the  $\rho$  mesons respectively. The parameters of these interactions are then evaluated self-consistently by using the saturation properties like binding energy per nucleon, pressure, compressibility and the symmetry energy. The equation of state (EOS) of asymmetric nuclear matter is subsequently evaluated and compared with existing results of other independent approaches available in current literature. The EOS of pure neutron matter is then used to calculate the mass and radius of a neutron star. We organize the paper as follows: In Section II, we present the theoretical formalism of the asymmetric nuclear matter as outlined above. The results are presented and discussed in Section III. Finally, in the last section the concluding remarks are drawn indicating the future outlook of the model.

## II. FORMALISM

The Lagrangian for the pion nucleon system is taken as

$$\mathcal{L} = \bar{\psi} (i\gamma^\mu \partial_\mu - M - G\gamma_5\varphi) \psi - \frac{1}{2} (\partial_\mu \varphi_i \partial^\mu \varphi_i - m^2 \varphi_i \varphi_i), \quad (1)$$

where  $\psi$  stands for the nucleon field with mass  $M$ ,  $\phi = \tau_i \phi_i$  represents the off-mass shell isospin triplet pion field with mass  $m$ ,  $\tau_i$  and  $\gamma^\mu$  being the isospin and Dirac matrices respectively,  $\gamma_5 = \begin{pmatrix} 0 & -i \\ -i & 0 \end{pmatrix}$  and  $G$  is the pion-nucleon coupling constant. Repeated indices indicate summation. As shown in [35, 36], we reduce the Lagrangian of equation(1) into its non-relativistic limit and the effective Hamiltonian becomes

$$\mathcal{H}(\mathbf{x}) = \mathcal{H}_N(\mathbf{x}) + \mathcal{H}_{int}(\mathbf{x}) + \mathcal{H}_M(\mathbf{x}), \quad (2)$$

where the free nucleon part  $\mathcal{H}_N(\mathbf{x})$  is given by

$$\mathcal{H}_N(\mathbf{x}) = \psi^\dagger(\mathbf{x}) \epsilon_x \psi(\mathbf{x}), \quad (3)$$

the free meson part  $\mathcal{H}_M(\mathbf{x})$  is defined as

$$\mathcal{H}_M(\mathbf{x}) = \frac{1}{2} [\dot{\varphi}_i^2 + (\nabla \varphi_i) \cdot (\nabla \varphi_i) + m^2 \varphi_i^2], \quad (4)$$

and the  $\pi N$  interaction [35] is provided by

$$\mathcal{H}_{int}(\mathbf{x}) = \psi^\dagger(\mathbf{x}) \left[ -\frac{iG}{2\epsilon_x} \boldsymbol{\sigma} \cdot \mathbf{p} \varphi + \frac{G^2}{2\epsilon_x} \varphi^2 \right] \psi(\mathbf{x}). \quad (5)$$

In equation (3),  $\psi$  represents the non-relativistic two component spin-isospin quartet nucleon field and the single particle nucleon energy operator  $\epsilon_x$  is given by  $\epsilon_x = (M^2 - \nabla_x^2)^{1/2}$ .

We expand the pion field operator  $\varphi_i(\mathbf{x})$  in terms of the creation and annihilation operators of off-mass shell pions satisfying equal time algebra as

$$\varphi_i(\mathbf{x}) = \frac{1}{\sqrt{2\omega_x}} (a_i(\mathbf{x})^\dagger + a_i(\mathbf{x})), \quad \dot{\varphi}_i(\mathbf{x}) = i\sqrt{\frac{\omega_x}{2}} (a_i(\mathbf{x})^\dagger - a_i(\mathbf{x})) \quad (6)$$

with energy  $\omega_x = (m^2 - \nabla_x^2)^{1/2}$  in the perturbative basis. We continue to use the perturbative basis, but note that since we take an arbitrary number of pions in the unitary transformation  $U$  in equation (8) as given later, the results would be nonperturbative. The two pions in eq. (5) provide a isoscalar scalar interaction of nucleons and thus would

simulate the effects of  $\sigma$ -mesons. A pion-pair creation operator given as

$$B^\dagger = \frac{1}{2} \int f(\mathbf{k}) a_i(\mathbf{k})^\dagger a_i(-\mathbf{k})^\dagger d\mathbf{k}, \quad (7)$$

is then constructed with the creation and annihilation operators in momentum space and the ansatz function  $f(\mathbf{k})$  which is to be determined later through a variational procedure.

We then define the unitary transformation  $U$  as

$$U = e^{(B^\dagger - B)} \quad (8)$$

and note that  $U$ , operating on vacuum, creates an arbitrarily large number of scalar isospin singlet pairs of pions. The ‘‘pion dressing’’ of nuclear matter is then introduced through the state

$$|f\rangle = U|vac\rangle = e^{(B^\dagger - B)}|vac\rangle. \quad (9)$$

Next, we define the operator  $U(\lambda)$  with an arbitrary parameter  $\lambda$  as  $U(\lambda) = e^{\lambda(B^\dagger - B)}$  and the function  $F(\mathbf{k}, \lambda)$  as  $F(\mathbf{k}, \lambda) = U^\dagger(\lambda) a(\mathbf{k}) U(\lambda)$ . Differentiating  $F(\mathbf{k}, \lambda)$  twice with respect to  $\lambda$ , we have the equation

$$\frac{d^2 F(\mathbf{k}, \lambda)}{d\lambda^2} = f^2(\mathbf{k}) F(\mathbf{k}, \lambda). \quad (10)$$

Solving the equation (10), and identifying  $\alpha(\mathbf{k}) = F(\mathbf{k}, \lambda = 1)$  we obtain

$$\alpha_i(\mathbf{k}) = U^\dagger a_i(\mathbf{k}) U = (\cosh f(\mathbf{k})) a_i(\mathbf{k}) + (\sinh f(\mathbf{k})) a_i(-\mathbf{k})^\dagger, \quad (11)$$

which is a Bogoliubov transformation. It can be easily checked that the operator  $\alpha(\mathbf{k})$  satisfies the standard bosonic commutation relations:

$$[\alpha_i(\mathbf{k}), \alpha_j^\dagger(\mathbf{k}')] = \delta_{ij} \delta(\mathbf{k} - \mathbf{k}'), \quad [\alpha_i^\dagger(\mathbf{k}), \alpha_j^\dagger(\mathbf{k}')] = [\alpha_i(\mathbf{k}), \alpha_j(\mathbf{k}')] = 0. \quad (12)$$

We then proceed to calculate the energy expectation values. We consider  $N$  nucleons occupying a spherical volume of radius  $R$  such that the density  $\rho = N/(\frac{4}{3}\pi R^3)$  remains constant as  $(N, R) \rightarrow \infty$  and we ignore the surface effects. We describe the system with a density operator  $\hat{\rho}_N$  such that its matrix elements are given by [35]

$$\rho_{\alpha\beta}(\mathbf{x}, \mathbf{y}) = Tr[\hat{\rho}_N \psi_\beta(\mathbf{y})^\dagger \psi_\alpha(\mathbf{x})], \quad (13)$$

and

$$Tr[\hat{\rho}_N \hat{N}] = \int \rho_{\alpha\alpha}(\mathbf{x}, \mathbf{x}) d\mathbf{x} = N = \rho V. \quad (14)$$

We obtain the free nucleon energy density

$$h_f = \langle f | Tr[\hat{\rho}_N \mathcal{H}_N(\mathbf{x})] | f \rangle = \sum_{\tau=n,p} \frac{\gamma k_f^\tau{}^3}{6\pi^2} \left( M + \frac{3}{10} \frac{k_f^\tau{}^2}{M} \right). \quad (15)$$

In the above equation, spin degeneracy factor  $\gamma = 2$ , the index  $\tau$  runs over the isospin degrees of freedom  $n, p$  and  $k_f^\tau$  represents the Fermi momenta of the nucleons. For asymmetric nuclear matter, we define the neutron and proton densities  $\rho_n$  and  $\rho_p$  respectively over the same spherical volume such that the nucleon density  $\rho = \rho_n + \rho_p$ . The Fermi momenta  $k_f^\tau$  and the nucleon densities are related by  $k_f^\tau = (6\pi^2 \rho_\tau / \gamma)^{\frac{1}{3}}$ . We also define the asymmetry parameter  $y = (\rho_n - \rho_p) / \rho$ . It can be easily seen that the nucleon densities  $\rho_\tau = \frac{\rho}{2}(1 \pm y)$  for  $\tau = n, p$  respectively.

Using the operator expansion of equation (6), the free pion part of the Hamiltonian as given in equation (4) can be written as

$$\mathcal{H}_M(\mathbf{x}) = a_i(\mathbf{x})^\dagger \omega_x a_i(\mathbf{x}). \quad (16)$$

This part represents the contribution due to kinetic energy of the pions to the total energy of the system. The free

pion kinetic energy density is given by

$$h_k = \langle f | \mathcal{H}_M(\mathbf{x}) | f \rangle = \frac{3}{(2\pi)^3} \int d\mathbf{k} \omega(\mathbf{k}) \sinh^2 f(\mathbf{k}), \quad (17)$$

where  $\omega(\mathbf{k}) = \sqrt{\mathbf{k}^2 + m^2}$ . In order to calculate the interaction energy density  $h_{int}$  in the non-relativistic limit, we have, from equation (5) using  $\epsilon_x \simeq M$

$$h_{int} = \langle f | Tr[\hat{\rho}_N \mathcal{H}_{int}(\mathbf{x})] | f \rangle \simeq \frac{G^2 \rho}{2M} \langle f | : \varphi_i(\mathbf{x}) \varphi_i(\mathbf{x}) : | f \rangle. \quad (18)$$

Using the equations (8), (9) and (11), we have from equation (18)

$$h_{int} = \frac{G^2 \rho}{2M} \left( \frac{3}{(2\pi)^3} \int \frac{d\mathbf{k}}{\omega(\mathbf{k})} \left( \frac{\sinh 2f(\mathbf{k})}{2} + \sinh^2 f(\mathbf{k}) \right) \right). \quad (19)$$

The pion field dependent energy density terms add up to give

$$h_m = h_k + h_{int}. \quad (20)$$

Now extremising equation (20) with respect to  $f(\mathbf{k})$ , we determine the ansatz function

$$\tanh 2f(\mathbf{k}) = -\frac{G^2 \rho}{2M} \frac{1}{\omega^2(\mathbf{k}) + \frac{G^2 \rho}{2M}}. \quad (21)$$

However, we note that this ansatz function yields a divergent value for  $h_m$ . This happens because we have taken the pions to be point like and have assumed that they can approach as near each other as they like, which is physically inaccurate. If we bring two pions close to each other there will be an effective force of repulsion because of their composite structure. We therefore replace the denominator in equation (21) by an additional term and rewrite the equation (21) as

$$\tanh 2f(\mathbf{k}) = -\frac{G^2 \rho}{2M} \cdot \frac{1}{\omega^2(\mathbf{k}) + \frac{G^2 \rho}{2M} + a\omega(\mathbf{k})e^{R_\pi^2 k^2}}. \quad (22)$$

The introduced term in the above expression for the ansatz  $f(\mathbf{k})$  corresponds to a phenomenological repulsion energy between the pions of a ‘‘pair’’ given by

$$h_m^R = \frac{3a}{(2\pi)^3} \int (\sinh^2 f(\mathbf{k})) e^{R_\pi^2 k^2} d\mathbf{k}, \quad (23)$$

where the two parameters  $a$  and  $R_\pi$  correspond to the strength and length scale, respectively, of the repulsion and are to be determined self-consistently later. Thus the pion field dependent terms of the energy density becomes  $h_m = h_k + h_{int} + h_m^R$  which is then evaluated as

$$h_m = -\frac{3}{2} \frac{1}{(2\pi)^3} \left( \frac{G^2}{2M} \right)^2 \rho \left[ \rho_n I_n + \rho_p I_p \right]. \quad (24)$$

In the above equation, the integrals  $I_\tau$  ( $\tau = n, p$ ) are given by

$$I_\tau = \int_0^{k_f^\tau} \frac{4\pi k^2 dk}{\omega^2} \cdot \left[ \frac{1}{(\omega + ae^{R_\pi^2 k^2})^{1/2} (\omega + e^{R_\pi^2 k^2} + \frac{G^2 \rho}{M\omega})^{1/2} + (\omega + e^{R_\pi^2 k^2}) + \frac{G^2 \rho}{2M\omega}} \right], \quad (25)$$

where  $\omega = \omega(\mathbf{k})$ .

The short range repulsion between the nucleons is known to be mediated by the isoscalar vector  $\omega$  mesons. Here we introduce the energy of repulsion by the simple form

$$h_\omega = \lambda_\omega \rho^2, \quad (26)$$

where the parameter  $\lambda_\omega$  is to be fixed using the saturation properties of nuclear matter as described later. We note

that equation (26) can arise from a Hamiltonian density given in terms of a local potential  $v_R(\mathbf{x})$  as

$$\mathcal{H}_R(\mathbf{x}) = \psi(\mathbf{x})^\dagger \psi(\mathbf{x}) \int v_R(\mathbf{x} - \mathbf{y}) \psi(\mathbf{y})^\dagger \psi(\mathbf{y}) d\mathbf{y}, \quad (27)$$

where, when density is constant, we in fact have

$$\lambda_\omega = \int v_R(\mathbf{x}) d\mathbf{x}.$$

The isospin dependent interaction is mediated by the isovector vector  $\rho$  mesons. We represent the contribution due to this interaction, in a manner similar to the  $\omega$ -meson energy, by the term

$$h_\rho = \lambda_\rho \rho_3^2 \quad (28)$$

where  $\rho_3 = (\rho_n - \rho_p)$  and the parameter  $\lambda_\rho$  is to be determined self consistently as described below.

Thus we finally write down the binding energy per nucleon  $E_B$  of the cold asymmetric nuclear matter:

$$E_B = \frac{\varepsilon}{\rho} - M \quad (29)$$

where  $\varepsilon = (h_m + h_f + h_\omega + h_\rho)$  is the energy density. The expression for  $\varepsilon$  contains the four model parameters  $a$ ,  $R_\pi$ ,  $\lambda_\omega$  and  $\lambda_\rho$  as introduced above. These parameters are then determined self-consistently through the saturation properties of nuclear matter. The pressure  $P$ , compressibility modulus  $K$  and the symmetry energy  $E_{sym}$  are given by the standard relations:

$$P = \rho^2 \frac{\partial(\varepsilon/\rho)}{\partial\rho} \quad (30)$$

$$K = 9\rho^2 \frac{\partial^2(\varepsilon/\rho)}{\partial\rho^2} \quad (31)$$

$$E_{sym} = \left( \frac{1}{2} \frac{\partial^2(\varepsilon/\rho)}{\partial y^2} \right)_{y=0}. \quad (32)$$

The effective mass  $M^*$  is given by  $M^* = M + V_s$  with  $V_s = (h_{int} + h_m^R)/\rho$ .

### III. RESULTS AND DISCUSSION

We now discuss the results obtained in our calculations and compare our results with those available in literature. The parameters of the model are fixed by self consistently solving eqs. (29-32) for the respective properties of nuclear matter at saturation density  $\rho_0 = 0.15 \text{ fm}^{-3}$ . The method used for solving the equations is the *globally convergent multidimensional Secant method* due to Broyden [39]. At saturation density, the values of binding energy per nucleon, pressure and symmetry energy are chosen to be -16 MeV, 0 and 31 MeV respectively. The value of compressibility modulus  $K$  at saturation density  $\rho_0$  is chosen to be 270 MeV following a procedure described below. The pion-nucleon coupling strength  $G^2/4\pi$ , the free nucleon mass  $M$  and the pion mass  $m$  are taken to be 14.6, 940.0 MeV and 140.0 MeV respectively.

In order to explore the parameter space substantively, we carry out the following process: First, we manually tune the parameter  $a$  and using Broyden's method variationally calculate the values of  $R_\pi$  and  $\lambda_\omega$ . Then, using these parameters in eq (31), we evaluate the compressibility  $K$ . In a similar way, next we tune  $R_\pi$  manually, while calculating variationally  $a$  and  $\lambda_\omega$ , and subsequently the compressibility  $K$ . In both of these parameter searches, we find that compressibility of the nuclear matter stabilizes around the value of 270 MeV. This also shows, as expected, that the value of  $\lambda_\omega$  is independent of the other parameters and is around the value of  $3.16 \text{ fm}^2$ . It also suggests that the values of  $a$  and  $R_\pi$  should be around 115 MeV and 1.06 fm respectively.

In order to further ascertain the dependence of compressibility modulus on the parameter values, we vary the  $K$  value over a range 210 MeV to 280 MeV and solve variationally for  $a$ ,  $R_\pi$  and  $\lambda_\omega$ . It may be noted that this is the range of the compressibility value which is under discussion in the current literature. For  $K$  values in the range 210 MeV to 250 MeV, the program does not converge. The solutions converge to stable parameter values only in the range 260 MeV to 280 MeV. The results obtained in this range for symmetric nuclear matter are presented in Table I. We choose  $K = 270 \text{ MeV}$  and the corresponding parameter values from Table I for our further studies. Finally we

generalise to asymmetric nuclear matter by fixing the symmetry energy at saturation density  $E_{sym}^0 = 31 \text{ MeV}$  in eq. (32) and by simultaneously solving the eqs. (29-32). The parameter values as shown in Table I remain unchanged in this process and we obtain  $\lambda_\rho = 0.650 \text{ fm}^2$ . As shown later, for this set of parameter values the effective mass of nucleons at saturation density is found to be  $M^*/M = 0.81$ .

TABLE I: Parameters of the model for symmetric nuclear matter evaluated for different  $K$  values in the range 260 MeV to 280 MeV. Value of saturation density  $\rho_0 = 0.15 \text{ fm}^{-3}$ .

K (MeV)	a (MeV)	$R_\pi$ (fm)	$\lambda_\omega$ (fm <sup>2</sup> )
260	17.00	1.424	3.098
265	57.28	1.207	3.131
270	115.26	1.061	3.164
275	205.15	0.922	3.199
280	367.88	0.756	3.237

The binding energy per nucleon  $E_B$  as a function of the density of the system is often referred to as the nuclear equation of state (EOS). In the Fig. 1, we present the EOS calculated for different values of the asymmetry parameter  $y$ . The values  $y = 0.0$  and  $1.0$  correspond to symmetric nuclear matter (SNM) and pure neutron matter (PNM) respectively. For SNM the binding energy, as expected, initially decreases with increase in density, reaches a minimum at  $\rho = \rho_0$  and then increases. In case of PNM, the binding energy increases monotonically with increasing density.

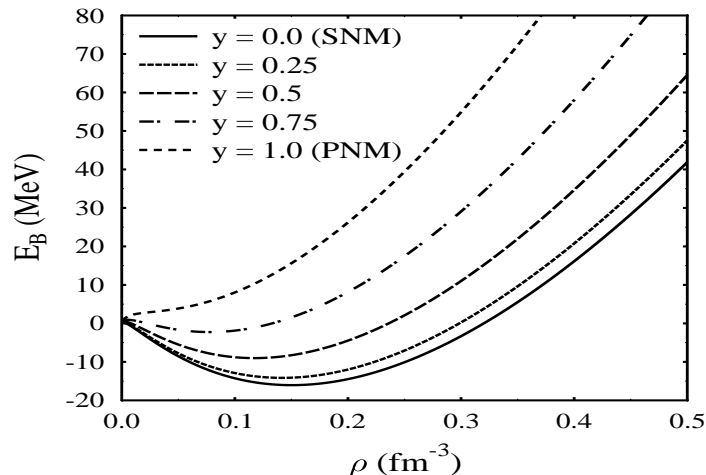


FIG. 1: The binding energy per nucleon  $E_B$  as a function of nucleon density  $\rho$  calculated for different values of the asymmetry parameter  $y$ . The values  $y = 0.0$  and  $1.0$  correspond to symmetric nuclear matter (SNM) and pure neutron matter (PNM) respectively.

In the Fig.2, we show the variation of the pressure  $P$  as a function of the energy density  $\varepsilon$ . For comparison, the causal limit  $P = \varepsilon$  is also shown in the figure. It is evident from this curve that our EOS is consistent with the causality condition  $\partial P/\partial\varepsilon \leq 1$ , so that the speed of sound remains lower than the speed of light.

Next, we present comparison of our results with the results of other groups available in the literature. In Fig. 3(a), we plot  $E_B$  as a function of the nucleon density  $\rho$  for the symmetric nuclear matter (SNM) along with results of the Walecka model [26] (long-short dashed curve), the DBHF calculations of Li *et al.* with Bonn A potential (short-dashed curve) (data for both the models are taken from [11]) and the variational A18 +  $\delta v$  + UIX\* (corrected) model of Argonne group [19] (long-dashed curve). While the Walecka and Bonn A models are relativistic, the variational model is nonrelativistic with relativistic corrections and three body correlations introduced successively. Our model produces an EOS softer than that of Walecka, but stiffer than the others. It is well-known that the Walecka model produces saturation of the nuclear matter properties correctly, though with a very high compressibility modulus of  $K = 540 \text{ MeV}$ . Our model yields nuclear matter saturation properties correctly alongwith the compressibility of  $K = 270 \text{ MeV}$

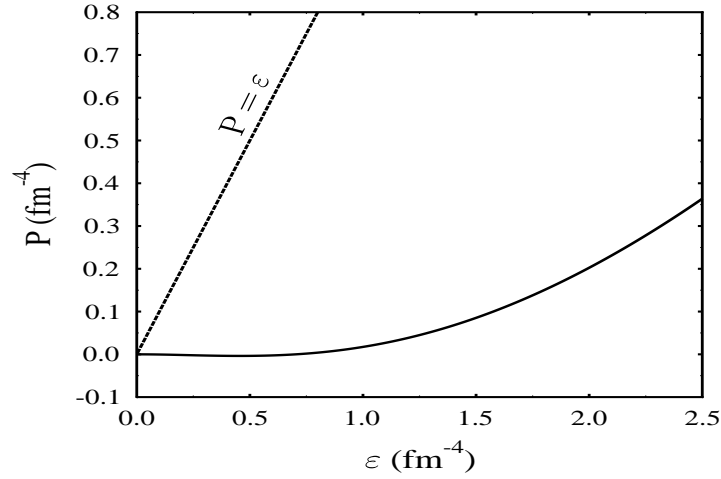


FIG. 2: The pressure  $P$  as a function of energy density  $\varepsilon$  for SNM. It is evident from this curve that our EOS respects the causality condition  $\partial P/\partial \varepsilon \leq 1$ , so that the speed of sound remains lower than the speed of light.

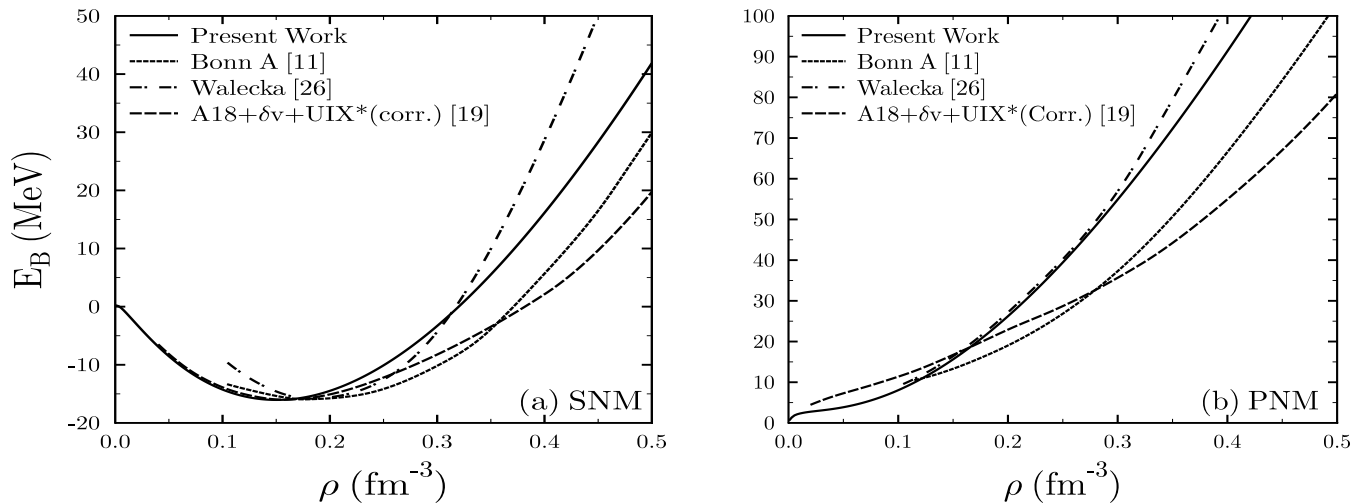


FIG. 3: Left panel: The binding energy per nucleon  $E_B$  as a function of nucleon density  $\rho$  for SNM. Our results are compared with results of DBHF calculations with Bonn A potential [11], Argonne group [19] and the Walecka model [26]. The data for the Bonn A and Walecka model curves are taken from [11].

Right panel: Same as 3(a), but for PNM.

which is reasonably close to the empirical data. In Fig. 3(b), we plot  $E_B$  as a function of the nucleon density  $\rho$  for PNM. Similar to the SNM case, our EOS is softer than that of Walecka model, but stiffer than those of Bonn A and the variational model. We use this EOS to calculate the mass and radius of a neutron star of PNM as discussed later.

The potentials per nucleon in our model can be defined from the meson dependent energy terms of eqs. (24), (26) and (28). Contribution to potential from the scalar part of the meson interaction is due to the pion condensates and is given by  $V_s = (h_{int} + h_m^R)/\rho$  as defined earlier. The contribution by vector mesons has two components, namely, due to the  $\omega$  and the  $\rho$  mesons and is given by  $V_v = V_\omega + V_\rho = (h_\omega + h_\rho)/\rho$ . In the Figs. 4, we plot  $V_s$  and  $V_v$  as functions of nucleon density  $\rho$  calculated for SNM (Fig. 4(a)) and for PNM (Fig. 4(b)) respectively. The magnitudes of the potentials calculated by our model are weaker compared to those produced by DBHF calculations with Bonn A interaction [11] as shown in both the panels of Fig. 4. In Fig. 4(b), we show the contributions to the repulsive vector potential due to  $\omega$  mesons (short-dashed curve),  $\rho$  mesons (long-dashed curve) and their combined contribution (long-short-dashed curve). The contribution due to  $\rho$  mesons rises linearly at a slow rate and has a low contribution at saturation density. This indicates that major contribution to the short-range repulsion part of nuclear force is from  $\omega$  meson interaction.

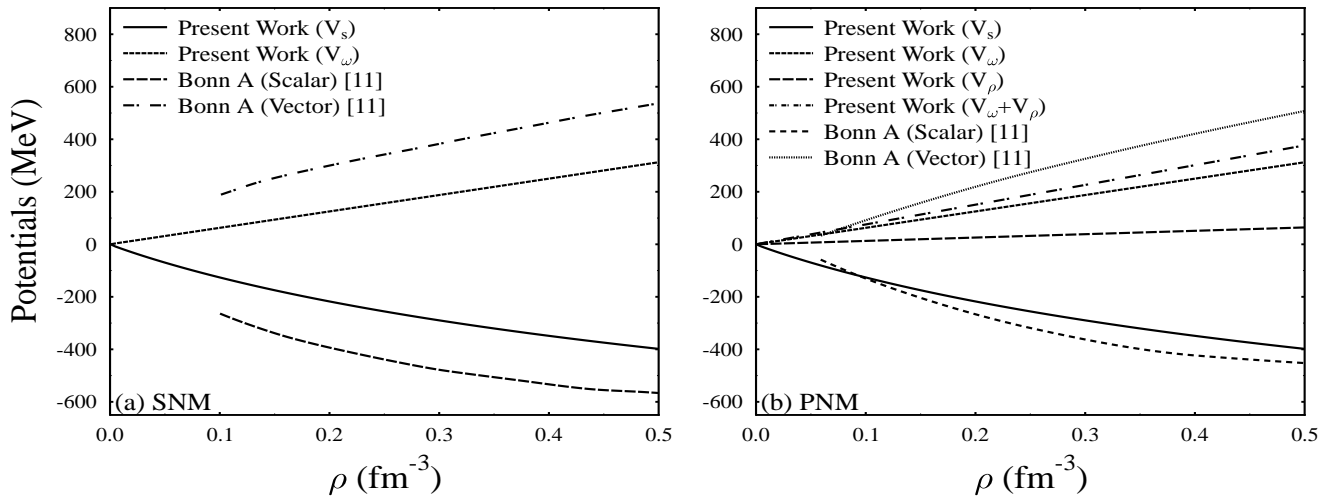


FIG. 4: Left panel: The potentials  $V_s$  and  $V_\omega$  (as defined in the text) in SNM calculated by our model are compared with those of the DBHF calculations with Bonn A potential [11]. Because of isospin symmetry,  $V_\rho$  (see text for definition) vanishes. Both the scalar (solid curve) and vector (short-dashed curve) potentials produced by our calculations are weaker in magnitude. Right panel: The potentials in PNM calculated by our model are compared with the Bonn A results of Li *et al.*[11]. The contributions made by the  $\omega$ -meson (short-dashed curve) and  $\rho$ -meson (long-dashed curve) mediated interactions are distinctly shown for comparison.

In Fig. 5, we present the effective mass  $M^*/M$  produced by our calculations (solid curve) and those with Bonn A interaction (short-dashed curve) and Walecka model (long-dashed curve) (data taken from [11]). As the effective mass has a contribution only from the scalar potential  $V_s$ , this property is independent of the asymmetry parameter  $y$ . The variation of  $M^*/M$  is slower in our case as compared to the Bonn A and the Walecka models. The empirical value for effective mass in nuclear matter derived from analysis of experimental data in the framework of non-relativistic shell or optical models is [7]  $M^*/M \simeq 0.7 - 0.8$ . We, however, get a slightly higher effective mass of  $M^*/M = 0.81$  at saturation density. This is due to lower contribution (in absolute terms) of the scalar interaction in the medium as shown in Fig. 5.

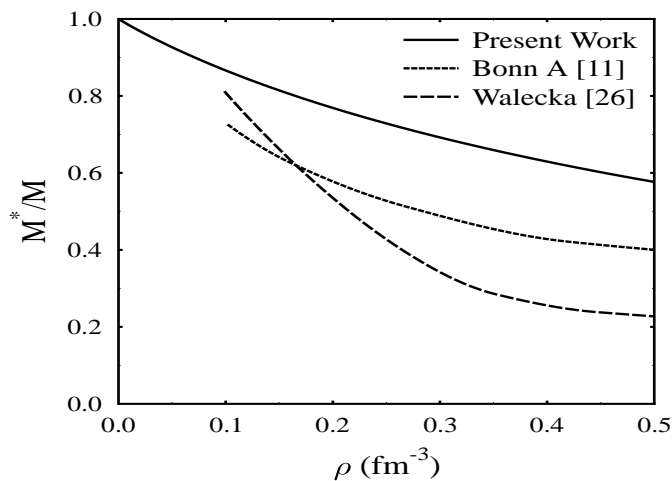


FIG. 5: The effective mass of nucleons (as defined in text) calculated by our model (solid curve) is compared with those of Bonn A (short-dashed) and Walecka model (long-dashed) curves (data taken from [11]). At saturation density the  $M^*/M$  value produced by our model is 0.81. A weaker potential  $V_s$  produces a higher  $M^*/M$  value in our calculations.

Knowledge of density dependence of symmetry energy is expected to play a key role in understanding the structure and properties of neutron-rich nuclei and neutron stars at densities above and below the saturation density. Therefore this problem has been receiving considerable attention of late. Several theoretical and experimental investigations



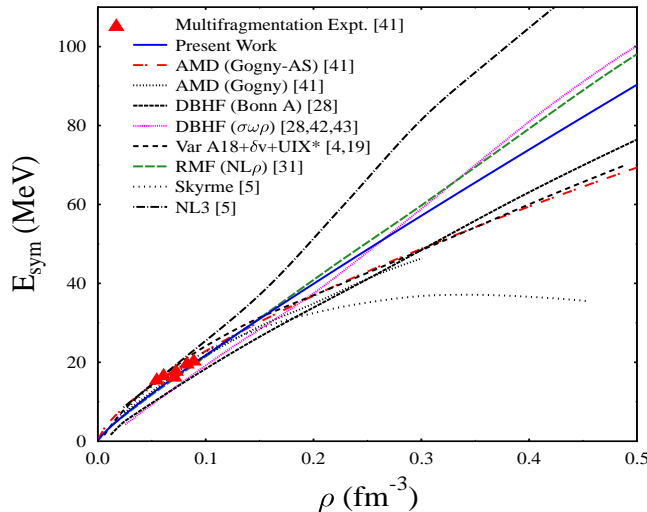


FIG. 6: Symmetry energy  $E_{sym}$  calculated from the EOS (as in Eq. 32) (solid blue line) is plotted along with results of other groups. The data for experimental points and the results of the antisymmetrized molecular dynamics (AMD) simulations with Gogny-AS and Gogny interactions are taken from Shetty *et al* [41], DBHF (Bonn A) results are taken from [28], RMF (NL $\rho$ ) data are from [31], the variational (A18+ $\delta v$ + UIX\*) model of Akmal *et al.* [19] results are from [4], DBHF ( $\sigma\omega\rho$ ) model of Huber *et al.* [42, 43] data are from [28], the Skyrme and NL3 results are from [5]. Our result shows consistency with those of other groups and corroborates the “stiff” dependence of  $E_{sym}$  as advocated by Shetty *et al.* [41].

addressing this problem have been reported ([4, 5, 41] and references therein). While the results of independent studies show reasonable consistency at sub-saturation densities  $\rho \leq \rho_0$ , they are at wide variance with each other at supra-saturation densities  $\rho > \rho_0$ . This wide variation has given rise to the so-called classification of “soft” and “stiff” dependence of symmetry energy on density [40, 41].

Fig. 6 shows a representation of the spectrum of such results along with the results of the present work (solid blue curve). While the Gogny and Skyrme forces (dark rib-dotted and dotted curves respectively with data taken from [5, 41]) produce “soft” dependence on one end, the NL3 force (dot-dashed curve with data taken from [5]) produces a very “stiff” dependence on the other end. The analysis of experimental and simulation studies of intermediate energy heavy-ion reactions as reported by Shetty *et al.* [41] (red triangles and long-short-dashed red curve respectively), results of DBHF calculations of Li *et al.* and Huber *et al.* [11, 28, 42, 43] (rib-dashed and magenta ribbed curve), variational model [4, 19] (short-dashed curve), RMF calculations with nonlinear Walecka model including  $\rho$  mesons by Liu *et al.* [31] (long-dashed green curve) as shown in Fig. 6 suggest “stiff” dependence with various degrees of stiffness. The experimental results (represented by the red triangles with data taken from Shetty *et al.* [41]) are derived from the isoscaling parameter  $\alpha$  which, in turn, is obtained from relative isotopic yields due to multifragmentation of excited nuclei produced by bombarding beams of  $^{58}\text{Fe}$  and  $^{58}\text{Ni}$  on  $^{58}\text{Fe}$  and  $^{58}\text{Ni}$  targets. Shetty *et al.* have shown that the results of multifragmentation simulation studies carried out with Antisymmetrized Molecular Dynamics (AMD) model using Gogny-AS interaction and Statistical Multifragmentation Model (SMM) are consistent with the above-mentioned experimental results and suggest (as shown by the red long-short-dashed curve) a moderately stiff dependence of the symmetry energy on density. Our results (represented by the solid blue curve) calculated using eqn. (32) are consistent with these results at subsaturation densities but are stiffer at supra-saturation densities. In Fig.6, the curve due to Huber *et al.* [42, 43] (with data taken from [28]) correspond to their DBHF ‘HD’ model calculations which involves only the  $\sigma$ ,  $\omega$  and  $\rho$  mesons. Similarly the long-dashed green curve due to Liu *et al.* [31] is from the basic non-linear Walecka model with  $\sigma$ ,  $\omega$  and  $\rho$  mesons. Our formalism is the closest to these two models with the exception that in our model the effect of  $\sigma$  mesons is simulated by the  $\pi$  meson condensates. It is also noteworthy that our results are consistent with these results for densities upto  $2\rho_0$ .

The wide variation of density dependence of symmetry energy at supra-saturation densities has given rise to the need of constraining it. As discussed by Shetty *et al* [41], a general functional form  $E_{sym} = E_{sym}^0 (\rho/\rho_0)^\gamma$  has emerged. Studies by various groups have produced the fits with  $E_{sym}^0 \sim 31 - 33$  MeV and  $\gamma \sim 0.55 - 1.05$ . A similar parametrization of the  $E_{sym}$  produced by our EOS with  $E_{sym}^0 = 31$  MeV yields the exponent parameter  $\gamma = 0.85$ . In Fig. 7, the symmetry energy calculated directly from the EOS by eqn. (32) (solid curve) and by the fit (dashed curve) are presented.

We next use the equation of state for PNM derived by our model in the Tolman-Oppenheimer-Volkoff (TOV) equation to calculate the mass and radius of a PNM neutron star. In Fig. 8 we show the neutron star mass as a

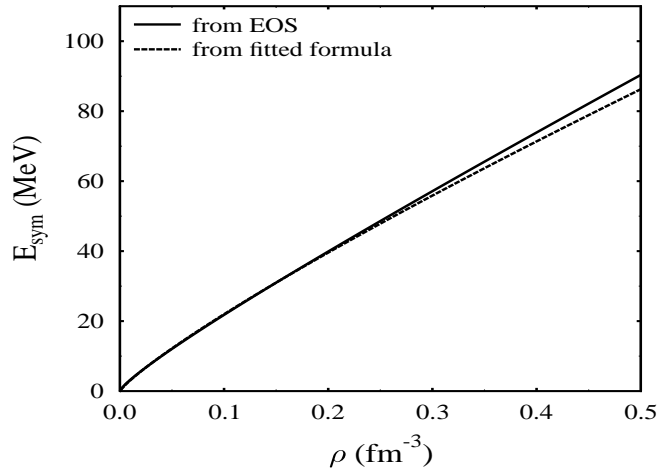


FIG. 7: Density dependence of the symmetry energy  $E_{sym}$  as calculated from the EOS using eqn. (32) (solid curve, same as the blue solid line of Fig. 6) and from parametric fit  $E_{sym} = E_{sym}^0(\rho/\rho_0)^\gamma$  with  $E_{sym}^0 = 31$  MeV and  $\gamma = 0.85$  (dashed) are plotted.

function of its radius as obtained from the TOV equation. The mass and radius of the star are found to be  $2.25 M_\odot$  and 11.7 km respectively. In the Fig. 9 we show the neutron star mass as a function of its central energy density  $\varepsilon_c$ . We observe that as  $\varepsilon_c$  increases the mass of the star increases first but eventually reaches the Chandrasekher limit.

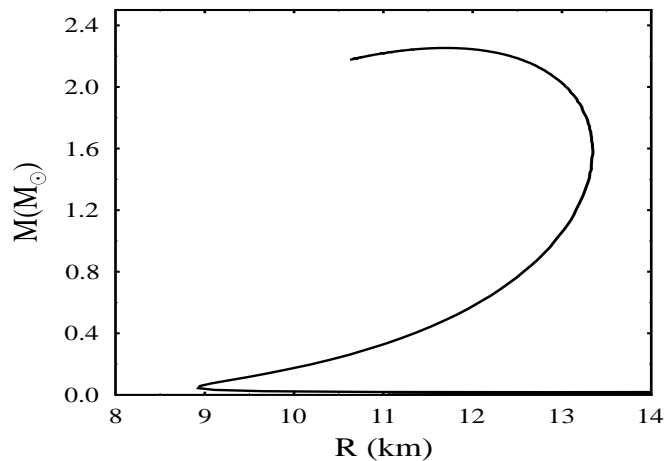


FIG. 8: Mass of a PNM neutron star (in units of solar mass  $M_\odot$ ) produced by our EOS as a function of radius. Maximum mass of the star turns out to be  $2.25 M_\odot$  with a radius of 11.7 km.

#### IV. CONCLUSION

In this work we have presented a quantum mechanical nonperturbative formalism to study cold asymmetric nuclear matter using a variational method. The system is assumed to be a collection of nucleons interacting via exchange of  $\pi$  pairs,  $\omega$  and  $\rho$  mesons. The equation of state (EOS) for different values of asymmetry parameter is derived from the dynamics of the interacting system in a self-consistent manner. This formalism yields results similar to those of the *ab initio* DBHF models, variational models and the RMF models without invoking the  $\sigma$  mesons. The compressibility modulus and effective mass are found to be  $K = 270$  MeV and  $M^*/M = 0.81$  respectively. The symmetry energy calculated from the EOS suggests a “stiff” dependence at supra-saturation densities and corroborates the recent arguments of Shetty et al. [41]. A parametrization of the density dependence of symmetry energy of the form

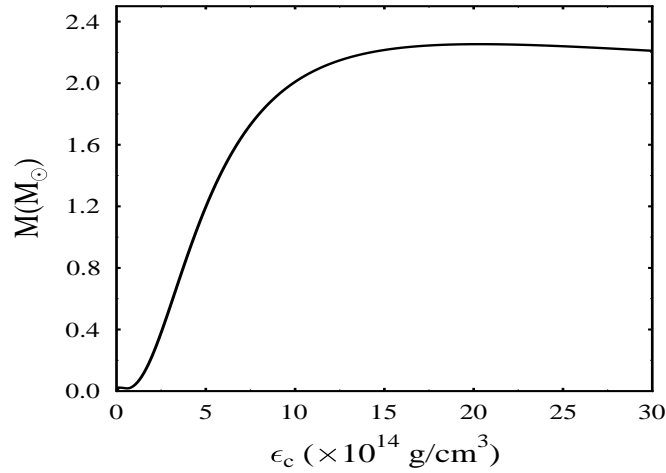


FIG. 9: Mass of a PNM neutron star as a function of the central energy density  $\epsilon_c$  is plotted. The mass of the star converges to Chandrasekhar limit.

$E_{sym} = E_{sym}^0(\rho/\rho_0)^\gamma$  with the symmetry energy  $E_{sym}^0$  at saturation density being 31 MeV produces  $\gamma = 0.85$ . The EOS of pure neutron matter (PNM) derived by the formalism yields the mass and radius of a PNM neutron star to be  $2.25 M_\odot$  and 11.7 km respectively.

Besides the aesthetic appeal, we note that the present formalism may also have experimental consequences. For example, the off shell  $\pi^+\pi^-$ -pair in the pion dressing may annihilate to hard photons with a probability in excess of what one may expect otherwise. Extension of the formalism to study asymmetric nuclear matter at finite temperature is currently under progress.

## V. ACKNOWLEDGEMENTS

The authors are thankful to Professor S.P. Misra for many useful discussions and for critically reading the manuscript.

- 
- [1] M. Prakash, I. Bombaci, M Prakash, P.J. Ellis, and J.M. Lattimer, *Phys. Rep.* **280**, 1 (1997).
  - [2] P.Danielewicz, R. Lacey and W.G. Lynch, *Science* **298**, 1592 (2002).
  - [3] J.M. Lattimer and M. Prakash, *Phys. Rep.* **333**, 121 (2000); *Astrophys. J.* **550**, 426 (2001); *Science* **304**, 536 (2004).
  - [4] A. W. Steiner, M. Prakash, J.M. Lattimer and P.J. Ellis, *Phys. Rep.* **441**, 325 (2005).
  - [5] C. Fuchs and H.H. Wolter, *Eur. Phys. J. A* **30**, 5 (2006).
  - [6] J.Margueron, E. van Dalen, C. Fuchs, *Phys. Rev. C* **76**, 034309 (2007).
  - [7] M. Jaminon and C. Mahaux, *Phys. Rev. C* **40**, 354 (1989).
  - [8] X.R. Zhou, G.F. Burgio, U. Lombardo, H.-J. Schulze, W. Zuo, *Phys. Rev. C* **69**, 018801 (2004).
  - [9] M.Baldo and C. Maieron, *J. Phys. G* **34**, R243 (2007).
  - [10] R. Brockmann and R. Machleidt, *Phys. Rev. C* **42**, 1965 (1990).
  - [11] G.Q. Li, R. Machleidt and R. Brockmann, *Phys. Rev. C* **45**, 2782 (1992).
  - [12] F. de Jong and H. Lenske, *Phys. Rev. C* **58**, 890 (1998).
  - [13] T. Gross-Boelting, C. Fuchs and A. Faessler, *Nucl. Phys. A* **648**, 890 (1999).
  - [14] E.N.E van Dalen, C. Fuchs and A. Faessler, *Nucl. Phys. A* **744**, 227 (2004); *Eur. Phys. J. A* **31**, 29 (2007).
  - [15] J. Carlson, J. Morales, V.R. Pandharipande, D.G. Ravenhall, *Phys. Rev. C* **68**, 025802 (2003).
  - [16] W.H. Dickhoff, C. Barbieri, *Prog. Part. Nucl. Phys.* **52**, 377 (2004).
  - [17] A. Fabrocini, S. Fantoni, A.Y. Illarionov and K.E. Schmidt, *Phys. Rev. Lett.* **95**, 192501 (2005).
  - [18] A. Akmal and V.R. Pandharipande, *Phys. Rev. C* **56**, 2261 (1997).
  - [19] A. Akmal, V.R. Pandharipande and D.G. Ravenhall *Phys. Rev. C* **58**, 1804 (1998).
  - [20] B.D. Serot, J.D. Walecka, *Int. J. Mod. Phys E* **6**, 515 (1997).
  - [21] R.J furnstahl, *Lect. Notes Phys.* **641**, 1 (2004)
  - [22] M. Lutz, B. Friman, Ch. Appel, *Phys. Lett B* **474**, 7 (2000).

- [23] P. Finelli, N. Kaiser, D. Vretenar, W. Weise, *Eur. Phys. J A* **17**, 573, (2003); *Nucl. Phys. A* **735**, 449 (2004).
- [24] M. Bender, P.-H. Heenen, P.-G. Reinhard, *Rev. Mod. Phys.* **75** 2003.
- [25] J.D. Walecka, *Ann. Phys.(N.Y.)* **83**, 491 (1974)
- [26] B.D. Serot and J.D. Walecka, *Adv. Nucl. Phys.***16**, 1 (1986).
- [27] P. Ring, *Prog. Part. Nucl. Phys.* **73**, 193 (1996); Y.K. Gambhir and P. Ring, *Phys. Lett.***B 202**, 2 (1988).
- [28] J.K. Bunta and Š. Gmuca, *Phys. Rev C* **68**, 054318 (2003); S. Gmuca, *J. Phys. G* **17**, 1115 (1991).
- [29] L. Brito, C. Providência, A.M. Santos, S.S. Avancini, D.P. menezes and Ph. Chomaz, *Phys. Rev C* **74**, 045801 (2006).
- [30] C. Providência, L. Brito, A.M. Santos, D.P. menezes, S.S. Avancini, *Phys. Rev. C* **74**, 045802 (2006).
- [31] B. Liu, M. D Toro, V. Greco, C. W. Shen, E. G. Zhao and B. X. Sun, e-print Arxiv No. nucl-th/0702064.
- [32] J. Meng, H. Toki, S.G. Zhou, S.Q. Zhang, W.H. Long and L.S. Geng, *Prog. Part. Nucl. Phys* **57**, 470 (2006)
- [33] K. Saito and A.W. Thomas, *Phys. Lett. B* **327**, 9 (1994); **335**, 17 (1994); **363**, 157 (1995); *Phys. Rev. C* **52**, 2789 (1995); P.A.M. Guichon, K. Saito, E. Rodionov, and A.W. Thomas, *Nucl. Phys. A***601** 349 (1996); P.K. Panda, A. Mishra, J.M. Eisenberg, W. Greiner, *Phys. Rev. C* **56**, 3134 (1997).
- [34] P.K. Panda, G. Krein, D.P. Menezes and C. Providência, *Phys. Rev. C* **68**, 015201 (2003).
- [35] A. Mishra, H. Mishra and S.P. Misra, *Int. J. Mod. Phys. A* **7**, 3391 (1990).
- [36] H. Mishra, S.P. Misra, P.K. Panda, B. K. Parida, *Int. J. Mod. Phys. E* **2**, 405 (1992).
- [37] P.K. Panda, S.P. Misra, R. Sahu, *Phys. Rev. C* **45**, 2079 (1992).
- [38] P.K. Panda, S.K. Patra, S.P. Misra, R. Sahu, *Int. J. Mod. Phys. E* **5**, 575 (1996).
- [39] W.H. Press, S.A. Teukolsky, W.T. Vetterling and B.P. Flannery, *Numerical recipes in FORTRAN: The Art of Scientific Programming* (Cambridge University Press, First Indian Edition, 1993).
- [40] J. R. Stone, J. C. Miller, R. Koncewicz, P.D. Stevenson, and M. R. Strayer, *Phys. Rev. C* **68**, 034324 (2003).
- [41] D.V. Shetty, S.J. Yennello and G.A. Souliotis, *Phys. Rev. C* **76**, 024606 (2007)
- [42] H. Huber, F. Weber, and M. K. Weigel, *Phys. Lett. B* **317**, 485 (1993).
- [43] H. Huber, F. Weber, and M. K. Weigel, *Phys. Rev. C* **51**, 1790 (1995).